Urban Forestry & Urban Greening 31 (2018) 204–211

Contents lists available at ScienceDirect

Urban Forestry & Urban Greening

journal homepage: www.elsevier.com/locate/ufug

Shade factors for 149 taxa of in-leaf urban trees in the USA

E. Gregory McPherson[a,*,1], Qingfu Xiao[b], Natalie S. van Doorn[c], Nels Johnson[c], Shannon Albers[d], Paula J. Peper[c,1]

[a] USDA Forest Service, Pacific Southwest Research Station, 1731 Research Park Dr., Davis, CA, 95616, United States
[b] Department of Land, Air & Water Resources, University of California, Davis, United States
[c] USDA Forest Service, Pacific Southwest Research Station, United States
[d] Department of Plant Sciences, University of California, Davis, United States

ARTICLE INFO

Keywords:
Canopy analysis
Crown density
Digital images
Gap fraction
Leaf area
Tree shade
Urban forest

ABSTRACT

Shade factors, defined as the percentage of sky covered by foliage and branches within the perimeter of individual tree crowns, have been used to model the effects of trees on air pollutant uptake, building energy use and rainfall interception. For the past 30 years the primary source of shade factors was a database containing values from 47 species. In most cases, values were obtained from measurements on a single tree in one location. To expand this database 11,024 shade factors were obtained for 149 urban tree species through a photometric process applied to the predominant species in 17 U.S. cities. Two digital images were taken of each tree, crowns were isolated, silhouette area defined and shade factors calculated as the ratio of shaded (i.e., foliage and woody material) pixels to total pixels within the crown silhouette area. The highly nonlinear relationship between both age and diameter at breast height (DBH), and shade factor was captured using generalized additive mixed models.

We found that shade factors increased with age until trees reached about 20 years or 30 cm DBH. Using a single shade factor from a mature tree for a young tree can overestimate actual crown density. Also, in many cases, shade factors were found to vary considerably for the same species growing in different climate zones. We provide a set of tables that contain the necessary values to compute shade factors from DBH or age with species and climate effects accounted for. This new information expands the scope of urban species with measured shade factors and allows researchers and urban foresters to more accurately predict their values across time and space.

1. Introduction

Growing interest in the ecosystem services provided by urban trees, such as energy effects, rainfall interception, carbon storage, and air pollutant uptake, is driving new investments in urban forests as green infrastructure (Berland and Hopton, 2014; Livesley et al., 2016; Zölch et al., 2017). Biometric research is measuring and modeling the characteristics of different tree species that influence their performance, such as diameter at breast height (DBH), crown size, and leaf area (Dahlhausen et al., 2016; McPherson and Peper, 2012; Semenzato et al., 2011; Yoon et al., 2013). One trait that has received relatively little study is the crown density of urban trees. Shade factor, defined as the percentage of sky covered by foliage and branches within the perimeter of individual tree crowns, can vary by species from about 60% to 95% when trees are in-leaf (McPherson, 1984). Shade factors are an important parameter in numerical models of urban forest biometrics and benefits. They are applied with crown parameters in regression equations to estimate tree leaf area, which is used to model air pollutant uptake (Nowak et al., 2008). Shade factors are used for modeling effects of tree shade on energy use by buildings and the efficiency of roof-mounted solar systems (Heisler, 1982; Thayer and Maeda, 1985). They are proxies for crown gap fraction, a variable used to model the amount of precipitation that falls unimpeded through the tree crown (Xiao et al., 2000).

Foresters have long studied the manner in which forests absorb, radiate, reflect, and transmit radiant energy and its effects on ecophysiological processes such as photosynthesis, evapotranspiration, and growth (Reifsnyder and Lull, 1965). Urban forest canopies can reduce the risk of heat stress to city dwellers by regulating the thermal environment (Kong et al., 2014). Tree crowns attenuate solar radiation and increase latent heat flux through evapotranspiration, which reduces air temperature (Thom et al., 2016). Their cooling effectiveness varies

* Corresponding author.
E-mail addresses: gmcpherson@fs.fed.us (E.G. McPherson), qxiao@ucdavis.edu (Q. Xiao), nvandoorn@fs.fed.us (N.S. van Doorn), nelsjohnson@fs.fed.us (N. Johnson), snalbers@ucdavis.edu (S. Albers), ppeper@surewest.com (P.J. Peper).
[1] Retired.

https://doi.org/10.1016/j.ufug.2018.03.001
Received 6 July 2017; Received in revised form 20 February 2018; Accepted 2 March 2018
Available online 12 March 2018
1618-8667/ Published by Elsevier GmbH.

by species and depends on crown size and density (e.g., leaf area index) growth rate, and stress tolerance (Rahman et al., 2015, 2017). Recent research has been identifying the thermal impact of trees in cities, with particular interest on the effects of evapotranspiration on air temperatures (Kong et al., 2016).

The authors are not aware of studies that have measured differences in attenuation of solar radiation among species during the past few decades. That work was prompted by the US oil crisis of 1979, which led to increased use of solar hot water systems and the need for solar access (Erley and Jaffe, 1979). Researchers began studying attenuation of sunlight in urban forests to select and locate trees for summer shade without blocking light to solar collectors (Heisler, 1986b). The techniques they used to measure crown density have changed as the technology evolved. Irradiance reductions by open growing city trees were first measured with pyranometers and light meters (Canton et al., 1993; Erley and Jaffe, 1979; Heisler, 1986a; Wilkinson et al., 1991). With the advent of portable computers, photographic approaches were adopted because large numbers of trees could be easily measured (Wagar and Heisler, 1986; Wilkinson et al., 1991). Photographs of tree crowns were taken, then scanned to measure relative transmission, or shading coefficient, a term first used in the building engineering literature (ASHRAE, 1989). Wilkinson (1991) found that there was no significant difference between shade factors for trees in full-leaf derived from photographic and photometric means. The photographic approach is used in this study.

Although photographic methods are quick and allow large numbers of trees to be studied, they have their limitations. Because these images are recording gaps in crowns, they are not a good measure of radiant energy reduction by trees (Heisler, 1982). Much of the radiation in shade is in a diffuse form rather than direct beam because of reflection off leaves and branches. Shade factors obtained from measuring gaps can underestimate the amount of radiation under a tree because the diffuse component is not included.

Patterson et al. (2011) found that side view photos offer a robust method for estimating shade factor. However, while a photograph of a crown taken at an angle of approximately 30° above the horizon captures the horizontal density of the crown in one direction, this value may not accurately capture the crown's density in other directions, or its vertical density. For example, closely spaced street trees can have crown's that are wider perpendicular to the street, and narrower parallel to the street due to competition from adjacent street trees. Shade factors recorded for only the widest dimension are likely to be greater than values for the narrowest dimension. Inaccuracies in measurements of horizontal density can influence modeling of tree shade on building energy performance when solar elevation angles are very high or low. Similarly, shade factors from horizontal images of species with high ratios of crown height to width (i.e., tall, narrow crowns) might underestimate their vertical densities. This issue could impact modeling rainfall interception when precipitation falls from above.

Shade factors typically range from 70% to 90% among species in-leaf. Results of 73 in-leaf measurements of shade factors were compiled for 47 different tree species located throughout the U.S. (McPherson, 1984). Values ranged from 62% for honey locust (*Gleditsia triacanthos inermis*) to 93% for littleleaf linden (*Tilia cordata*). But do differences in shade factors among species substantially effect their functional performance?

In a sensitivity analysis of tree shade effects on residential buildings in Tucson, AZ a 10% difference in shade factor (75%–85%) increased annual cooling savings by 2% (75–150 kWh) depending on building size and type of construction (McPherson and Dougherty, 1989). Overall savings were proportional to the amount of area shaded based on crown size and shape, as well as the shade factor of each species. Shade factors ranged from 70% to 90% for a simulation of species planted for building shade in Sacramento, CA (Simpson and McPherson, 1998). The simulations assumed a constant shade factor for each mature species. These studies indicate that shade factor can have a substantial influence on building cooling savings. Unfortunately, these studies did not measure effects for the full 30% range in shade factors among species, or for changes in density that might occur as trees mature.

A sensitivity analysis of factors influencing rainfall interception by individual trees found that interception loss was sensitive to gap fraction, where gap fraction is defined as the percentage of crown area normal to the direction of rainfall that allows rain drops to reach the ground unimpeded (Xiao et al., 2000). The amount of unimpeded throughfall was directly proportional to the gap fraction. Keeping other factors constant, a three-fold increase in gap fraction was estimated to decrease interception loss (i.e., evaporation) from 12.1 to 4.3%. Interception estimates were highly sensitive to gap fraction, along with leaf area index and surface storage capacity. Shade factor was used as a proxy for gap fraction in modeling rainfall interception by Sacramento's urban forest (Xiao et al., 1998). In their measurements of interception by two eucalypt species (*Eucalyptus* sp.), Livesley et al. (2014) measured gap fraction using four upward-looking digital images for each tree. Gap fraction varied between species (14% and 20%).

In i-Tree, a software package widely used to model air pollutant uptake by trees, leaf area estimates from the i-Tree regression equation (Nowak, 1996) are very sensitive to the shade factor value (Fig. 1). The average shade factor from the literature for hackberry (*Celtis occidentalis*) is 88% (McPherson, 1984). Given variability of ± 10% among individual hackberry trees, shade factors can range from 78% to 98%. The i-Tree equation predicts that leaf area is 374 m^2 with the 88% shade factor at 20 years. Leaf areas for the dense (98%) and open (78%) hackberry are estimated to be 633 m^2 and 221 m^2, respectively. The ± 10% change in shade factors results in a nearly three-fold difference in estimated leaf area.

In summary, shade factors are used to model tree leaf area and functions such as effects of tree shade on building energy performance and rainfall interception. The most extensive database of shade factors is over 30 years old and contains values for only 47 species (McPherson, 1984). Most urban forests contain many more taxa than this. Presumably, values for other species must be assigned to those missing based on taxonomic or structural similarity. The current modeling assumptions are that shade factors remain static over the tree's lifetime and do not change within a species due to effects of management practices and different climates. If differences within species and across tree ages and climate zones are insignificant, a single shade factor per species can be justified for modeling purposes. If differences exist as trees of the same species age, or for trees of the same species located in different climate zones, accurate modeling of shade factors for the same species may need to incorporate changes in crown density across time and space. Hence, the goal of this research is to develop a process for calculating shade factors based on user inputs, such as species, size, age, and climate zone. To achieve this goal we answer the following

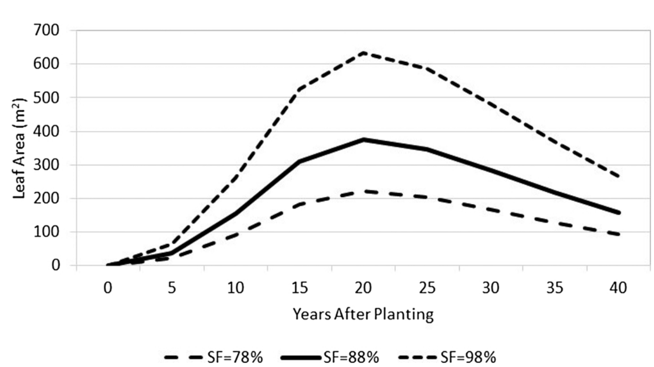

Fig. 1. Modeled leaf area of hackberry (*Celtis occidentalis*) using i-Tree's logarithmic regression equation (Nowak, 1996) and crown dimensions (height and diameter) from the Urban Tree Database (UTD) growth equations (McPherson et al., 2016). The sensitivity of leaf area to shade factors (SF) is illustrated using values that are ± 10% of the species average for hackberry (88%).

questions.

- What is the variability in shade factors for trees of the same species when considered across size and age?
- What is the variability in shade factors for trees of the same species when considered across climate zones?
- What is the variability in shade factors among species? Can species be categorized into shade factor classes, such as high, moderate, and low?

This study extends the current database of shade factors from about 50–149 taxa of urban trees, for the first time including palms and many subtropical evergreens. It uses statistical analyses to categorize species into classes such as high, moderate, and low shade factors. These data can be used for improved modeling of tree effects and for selecting species to achieve higher levels of performance.

2. Methods

2.1. Sampling design

Allometric equations for urban tree species have valuable uses, such as modeling size, growth, and biomass accumulation. However, their range of application and predictive power has been limited by small sample sizes, few species, young and excellent-condition trees only, and narrow geographic range. Research was conducted over a span of 14 years (1998–2011) to overcome some of these limitations. It resulted in 365 sets of allometric equations for the most abundant tree species in cities from around the United States (McPherson et al., 2016) and was incorporated into the i-Tree Streets (formerly Stratum) software (Maco and McPherson, 2003). Based on computerized street tree inventories and, occasionally hand-written documents, a stratified random sample of the most predominant 17–22 street tree species per reference city was selected (Peper et al., 2001). The term "reference city" refers to the city selected for intensive study within each of the 16 climate zones across the United States (Fig. 2) (McPherson, 2010). The sample was stratified into nine diameter at breast height (DBH) classes (0–7.6, 7.6–15.2, 15.2–30.5, 30.5–45.7, 45.7–61.0, 61.0–76.2, 76.2–91.4, 91.4–106.7, and > 106.7 cm). Typically 10–15 trees per DBH class were randomly chosen. Data were collected for 16–74 trees in total from each species.

Data collection took place in the late spring or summer when the trees were in full leaf. Measurements included: species name, age, DBH [to the nearest 0.1 cm (0.39 in)], tree height [to the nearest 0.5 m (1.64 ft.)], crown height [to the nearest 0.5 m (1.64 ft.)], and crown diameter in two directions [parallel and perpendicular to nearest street to the nearest 0.5 m (1.64 ft.)]. Tree age was determined from local residents, the city's urban forester, street and home construction dates, historical planting records, and aerial and historical photos. Two digital photographs were taken of the tree at 90° angles from one another at a distance that allowed for full capture of the crown. The distance of the camera to the bole was recorded to the nearest 1.5 m (5 ft.) using a Sonin electronic distance measuring tool (Peper and McPherson, 2003). Distances were recorded at regular intervals (i.e., 1.5, 3.0, 4.6, 6.1, 7.6, 9.1, 10.7, 12.2 m from the tree), as determined by the size of the tree crown and safety for the researcher. For example, if a tree could be photographed from 3.0 m away, but that placed the researcher in the middle of a busy intersection, the picture was taken from farther away for purposes of safety. Distances between the two images were not required to be the same and varied for the reasons mentioned above.

2.2. Image processing

2.2.1. Isolate tree crown

The crown of each tree was isolated using professional image editing software (Adobe Photoshop (version CS), https://www.adobe.com/products/photoshop.html). Digital camera make (i.e., Kodak DC50, Olympus D150, Nikon 900), model and image isolation software versions varied based on the year the capture and isolation analysis was performed. However, the format size ratio for all camera image sensors was 3:2, insuring images conformed to a 35 mm negative size without cropping or distortion (Peper and McPherson, 1998). During the crown isolation procedure, the background and the section of the bole beneath the lowest branches were removed in Photoshop using the "magic wand" and "lasso" tools.

2.2.2. Measure pixel size

To measure the crown dimensions the pixel size was required for each image. To measure pixel size an object of known size or a "reference board" was developed. This cardboard square (0.5 × 0.5 m) was photographed at the same distances used in the field to acquire the tree crown images. The pixel size of the image for each distance was calculated as the ratio of the reference board's total number of pixels on the image to the actual area of the reference board. The resulting pixel dimension values were converted to centimeters so that they could be used to obtain crown dimensions.

2.2.3. Create binary image files

Tree leaves and branches were manually set to black and the background was set to white using the grayscale feature in Photoshop (Fig. 3). The isolated tree crown image was opened in Photoshop and oriented to portrait. The color image was then rendered black and white (gaps). Natural gaps remained in the crown image where the sky or other background objects were previously removed. This binary image was saved in the raw image format as the "non-filled" version, named due to the natural gaps in the crown. The processer then returned to the black and white image, selected the background outside the tree crown, inversed the selection and deleted it. This process removed the background gaps that remained within the crown, making the tree crown solid black from the edges in. This image was saved in the raw image format as the "filled" version. These "non-filled" and "filled" files were used during batch file processing to calculate the crown characteristics.

2.2.4. Calculate shade factors

Shade factors were calculated as the ratio of the foliar and woody material pixels to total pixels within the crown silhouette area. The crown silhouette area was defined by connecting the furthest end tips of the tree branches, where the distance between two adjacent tips was less than 50 cm. A computer program was developed by one of the authors to determine the outline of the crown silhouette. Pixel size data were used in this program to measure where the 50 cm connection point occurred. With this information, the program automatically connected the branch tips to form the crown silhouette. A batch file accessed the "non-filled" image, "filled" image, and the distance from the tree that the image was taken in the field. With these data it calculated the silhouette area, shaded area, and shade factor for each image and saved results to a text file. The text files, and isolated crown and crown silhouette area images were used for quality control, which involved identifying missing data and outliers.

2.2.5. Perform quality control

After the batch file results were obtained the shade factors from each tree were matched to the corresponding photograph from the data collection workbook in each city. A quality control assessment was performed to identify anomalous values or trees without shade factors. Trees were removed from the database if both images were missing. For trees missing one image, the first and only image was duplicated so that there were two images for each tree. Shade factors were calculated as the average of the values of the two images for each tree. These values were then compiled in the master database so that shade factors could be compared across climate zones by species, size, and age. We identified anomalous values for approximately 300 trees. The cause for each

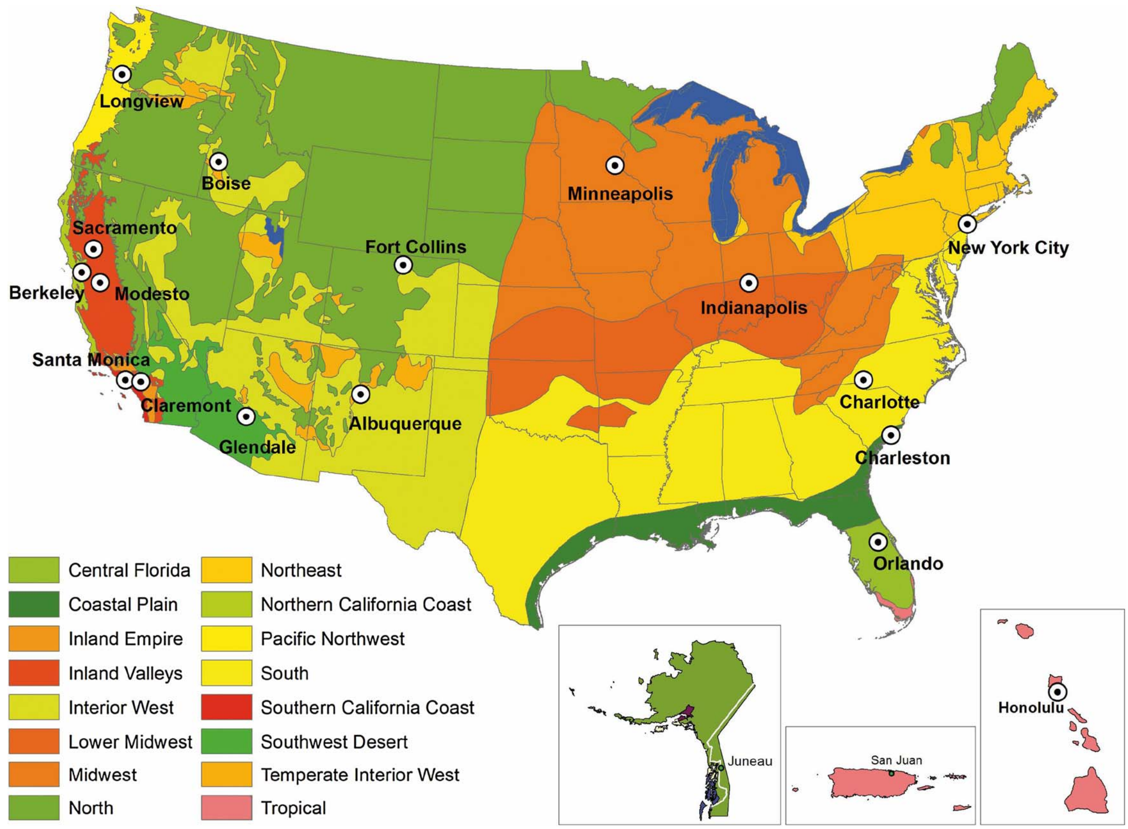

Fig. 2. Climate zones of the United States and Puerto Rico were aggregated from 45 Sunset climate zones into 16 zones. Each zone has a reference city where tree data were collected. Sacramento, California was added as a second reference city (with Modesto) to the Inland Valleys zone. Zones for Alaska, Puerto Rico and Hawaii are shown in the insets (map courtesy of Pacific Southwest Research Station).

value was identified by examining the isolated crown images and noted (e.g., defoliation, topped). Trees with substantial crown damage, as often evidenced by shade factors less than 60%, accounted for about 2% of all trees in the database (12,771 trees before cleaning, 11,024 trees final). We elected to retain these trees for analysis because they comprise a representative sample of municipal forests. To only include healthy trees with full crowns would overestimate the actual amount of shade that trees provide.

2.3. Statistical analysis

All statistical analyses were performed in R statistical software version 3.3.3 (R Core Team, 2017). To capture the highly nonlinear relationship between both age and DBH, and shade factor, generalized additive models (GAMs) and generalized additive mixed models (GAMMs) were fit using the gamm functions in the mgcv package (Wood, 2003, 2004, 2006, 2011, 2016). The GAMs and GAMMs were fit with a normally distributed error distribution and an identity link function. Otherwise, default values were used. The full GAMM model has the following form:

$$\mathrm{SF}_{ijk} = \beta_0 + f_1(\mathrm{dbh}_{ijk}) + f_2(\mathrm{age}_{ijk}) + u_j + b_{jk} + \varepsilon_{ijk},$$
$$u_j \sim \mathrm{Normal}(0, \sigma_u^2),$$
$$b_{jk} \sim \mathrm{Normal}(0, \sigma_b^2),$$
$$\varepsilon_{ijk} \sim \mathrm{Normal}(0, \sigma_e^2),$$

where i indexes tree, j indexes species, and k indexes climate, f_1 and f_2 are unknown functions estimated using low-rank thin-plate splines in the mgcv R package, β_0 is the intercept, u_j is the random species effect with variance σ_u^2, b_{jk} is the random climate within species random effect with variance σ_b^2, and ε_{ijk} is the random error with variance σ_e^2. The GAM model is the same as the GAMM without the u_j and b_{jk} random effects.

Model selection was performed based on AIC selection (Akaike, 1974; Burnham and Anderson, 2002). Using the version corrected for small sample size, AICc, was unnecessary due to large sample size (11,024). For fixed effects, models considered had a low-rank thin-plate spline term for either DBH, age, or both additively. For each of the three combinations of fixed effects, four possible random effect combinations were investigated: no random effects, a random intercept for species, a random intercept for climate, or a random intercept for species and a random intercept for climate within species. Altogether, twelve models were investigated. Of those, two did not converge: 1) DBH and climate, and 2) DBH, age, and climate.

The best model based on AIC was used to make climate within species specific shade factor predictions at the median DBH for the corresponding species-climate combination. Using the normalmixEM function (McLachlan and Peel, 2000; Meng and Rubin, 1993) in the mixtools package (Benaglia et al., 2009), the predicted shade factors were then clustered into three shade classes (i.e., light, medium, dense shade) using a finite mixture model approach. This approach generates a probability of shade class membership for each species-climate combination. Thus, the combinations are assigned to the shade class with the highest associated membership probability.

3. Results and discussion

Scatterplots and histograms of the shade factor, dbh, and age data are contained in Fig. 4. We see that age and DBH follow a right skewed distribution, shade factors follow a left skewed distribution. There is a strong relationship between age and DBH (cor = 0.795).

The best model based on AIC was the model containing DBH, species, and climate within species (Table 1). The second best contained age, DBH, species, and climate within species. The third best contained

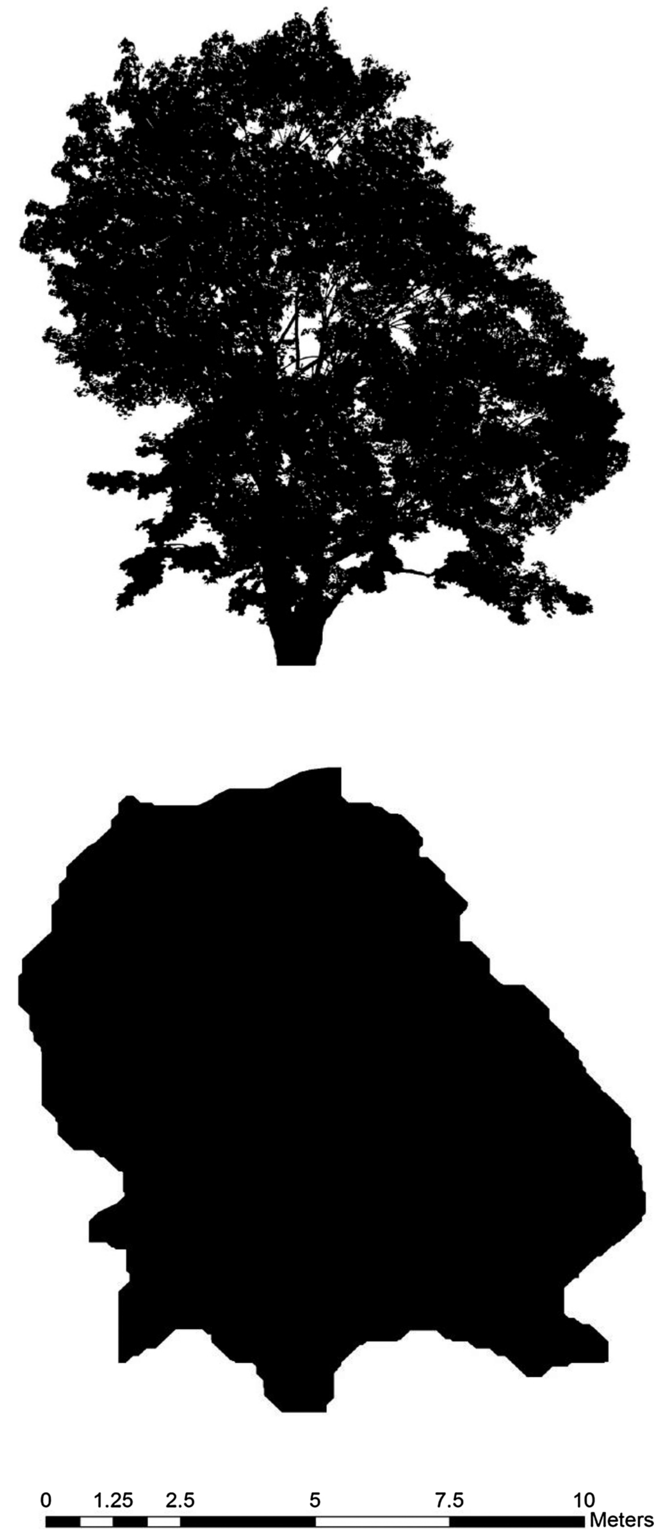

Fig. 3. Creating the binary image file first involved setting the isolated tree crown's background to white. In this "non-filled" image (top) of a Norway maple (*Acer platanoides*) the natural gaps in the crown remained white. In the "filled" image (below) the background outside the crown was selected, inversed and deleted. In effect, this step removed the gaps within the crown. This is the image used to define the crown silhouette area.

age, species, and climate within species. The estimated curve for DBH from the best model is shown in Fig. 5. The estimated curve for age from the third best model is shown in Fig. 6. We do not report the curves for the second best model, because in practice anyone with both age and DBH should use the DBH only model. The curves look very similar due to the large correlation between age and DBH (0.795), indicating they are both measuring nearly the same thing. There is a waviness of the curves for age and dbh that does not have any known scientific explanation. That could mean the waviness is an artefact of the low-rank thin-plate spline smoother used to estimate the curves. However, when we fit using other smoothing methods (results omitted), all had the same waviness. This leads us to believe that the waviness does really exist in the data as measured. Because all three top models included species and climate within species, we interpreted that the effect of climate depended on the species being considered. For example, shade factors changed considerably within a species based on the climate zone for *Gleditsia triacanthos*, *Malus species*, and *Ulmus parvifolia*. In contrast, they changed relatively little across climate zones for *Cinnamomum camphora*, *Fraxinus pennsylvanica,* and *Tilia americana*. Possible explanations for these observations are discussed later in this paper.

A smoothing spline approach was used to estimate the relationship between both age and DBH, and shade factor. As a result, there was no easy to use formula for computing shade factor from climate, species, and age/DBH. To compute shade factors, we provide a set of tables in the Supplementary Material that contain the necessary values from the models (Tables S1–S4). The process for calculating the shade factor for a particular combination of age/dbh, species, and climate is provided in the Supplemental Material. Table S5 contains the species-climate combinations associated with each shade density class. Table S6 provides the species code for each taxon and Table S7 provides the code for each climate zone.

The curves in Figs. 5 and 6 illustrate that shade factors tended to increase until trees reached about 20 years or 30 cm DBH. Hence, applying a shade factor from a mature tree to a young tree of the same species is apt to overestimate actual crown density. The initially steep rate of increase may correspond to the period after transplant stress when trees have high vitality and rapidly increase their crown volume. During this period of rapid growth, crown transparency decreases when viewed horizontally. Later in life trees often invest more resources in root development than in crown growth.

Fig. 7 contains violin plots of the weighted densities from the finite mixture model along with their associated shade factor values overlaid. Fig. 7 also contains estimates of the associated shade class weights, means, variances and associated range of shade factors, as well as the size of the shade class. Of the 298 species/climate combinations examined, 17 were light shade, 90 were medium and 191 were dense shade. The light shade class is the least populated with a wide potential range. The dense shade class is the most populated class with the smallest potential range. The medium shade class is between the light and dense shade classes with regards to size and potential range. A list of species-climate combination shade class membership is available in the Supplementary Material online (Table S5).

Our data indicate that it is not always possible to give a single shade factor for a species that occurs in multiple climate zones. For 30 species, the shade class changed within a species based on the climate zone. Four species (*Ginkgo biloba*, *Gleditsia triacanthos*, *Malus* sp., *Ulmus parvifolia*) were represented in each of the three shade classes. For example, honey locust were in the light (Coastal Plain region), medium (Inland Valleys), and dense shade classes (Interior West, Midwest, North, and Temperate Interior West). Three other species were found in both the light and medium shade classes and 23 others were in both the medium and dense shade classes. Although climate zone was found to be an important effect describing shade factor, not all species showed large variation in shade factor across climate zones. Shade factor changed relatively little across climate zones for species such as *Acer platanoides*, *Cinnamomum camphora*, *Fraxinus pennsylvanica, and Tilia americana*.

Different cultural practices may be partially responsible for cases where shade factors were found to vary considerably for the same

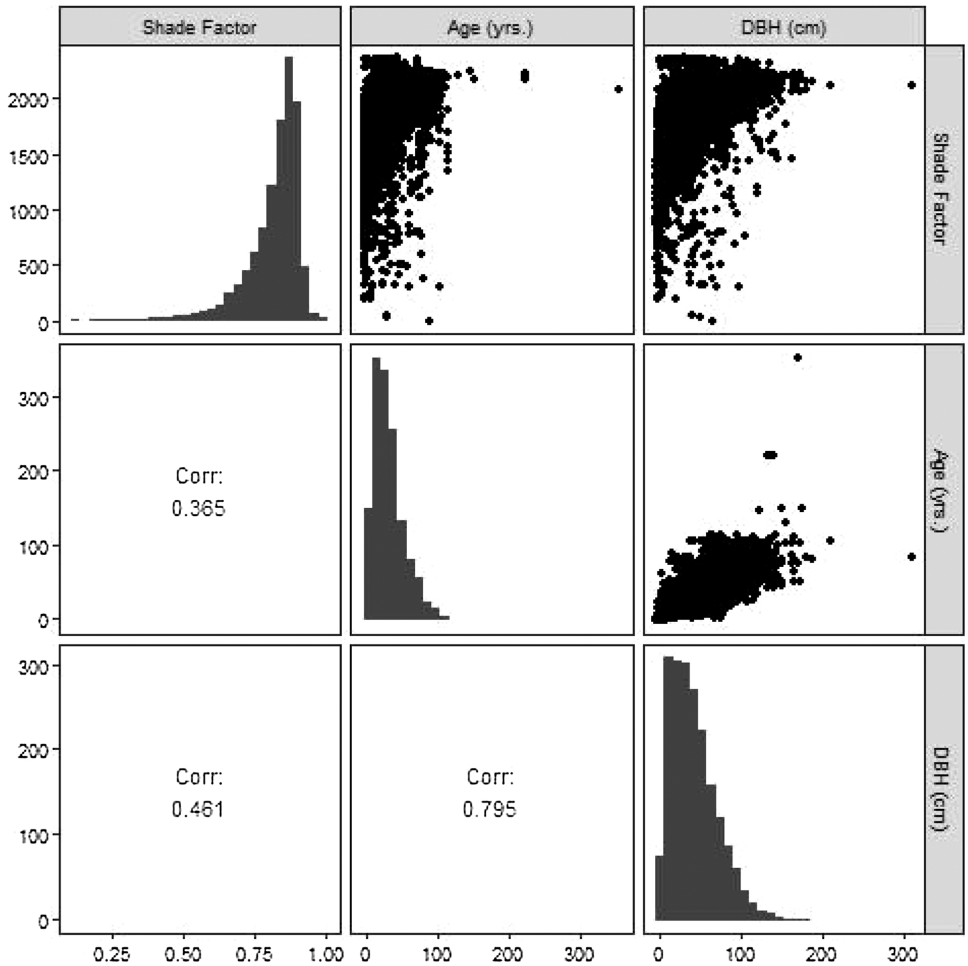

Fig. 4. Scatterplots and histograms of shade factor, age, and dbh.

species growing in different climate zones. For example, a study found that different pruning practices influenced growth and provisioning of ecosystem services by Siberian elms (*Ulmus pumila*) growing in San Francisco, CA and Cheyenne, Wyoming. Although the growing season was much longer in San Francisco than Cheyenne, the elms were much smaller and benefits were less than those from the same species in Cheyenne. Trees in San Francisco were extensively pruned to limit conflicts with buildings, roads, and overhead wires (McPherson and Peper, 2012). Pruning tends to invigorate vegetative growth and can eventually increase crown density if not taken to the extreme. Hence, shade factors can reflect species specific responses to pruning dose and frequency, which can vary from city to city.

Shade factors are one of many tree traits that influence energy effects. Tree species in the dense shade class (191 species/climate combinations) will provide greater air conditioning energy savings than will species in the light shade class (17), provided they are of similar size and location (McPherson and Dougherty, 1989; Simpson and McPherson, 1998). Crown area and its location relative to building surfaces are equally important to energy effects (Hwang et al., 2015, 2016). For example, dense shade on the roof from a crown raised above the wall may provide less cooling energy savings than a similar amount of lighter shade on the wall if the attic is thermally decoupled from the living space below by insulation, or the wall is largely single pane glazing.

Table 1
Table of AIC values for models of shade factor, sorted from best to worst, where the model with the smallest AIC is best. Also included are the estimated error standard deviation $\hat{\sigma}_e$, the intercept β_0, and random effect standard errors σ_u and σ_b. Asterisks denote models that did not converge. Double asterisks denote terms not estimated due to not being in the model.

Model	DF	AIC	Delta AIC	$\hat{\sigma}_e$	β_0	$\hat{\sigma}_u$	$\hat{\sigma}_b$
DBH, species, climate within species	6	−27380.21	0	0.067	0.83	8.2e-6	0.043
Age, DBH, species, climate within species	8	−26897.40	482.81	0.070	0.82	0.048	5.6e-5
Age, species, climate within species	6	−25731.81	1648.40	0.072	0.83	0.041	0.031
Age, species	5	−25094.12	2286.09	0.076	0.82	0.051	**
Age, climate	5	−24328.64	3051.56	0.080	0.83	**	0.033
Age, DBH	6	−24292.48	3087.73	0.080	0.83	**	**
Age, DBH, species	7	−24290.48	3089.73	0.080	0.83	9.0e-14	**
DBH	4	−24267.75	3112.46	0.080	0.83	**	**
DBH, species	5	−24265.75	3114.46	0.080	0.83	2.5e-14	**
Age	4	−22633.61	4746.59	0.086	0.83	**	**
DBH, climate	*	*	*	*	*	*	*
Age, DBH, climate	*	*	*	*	*	*	*

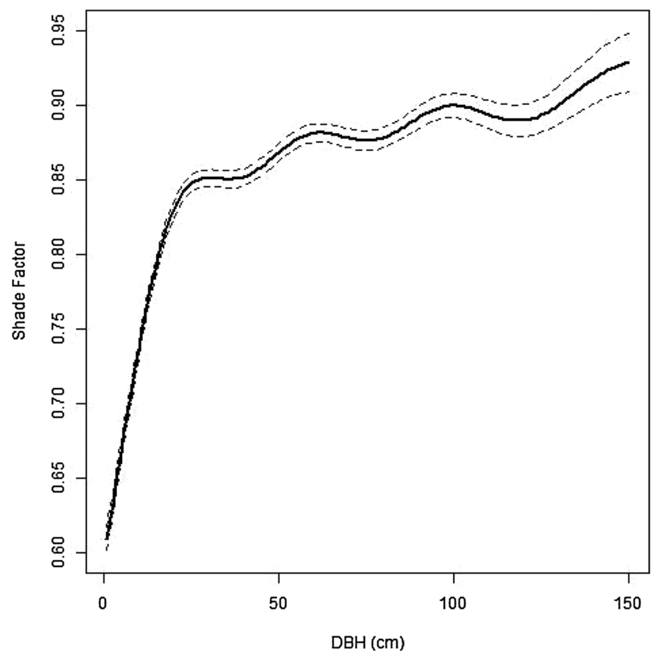

Fig. 5. Solid line is the low-rank thin-plate spline estimate of $f_1(\text{dbh}) + \beta_0$ from the model with DBH, species, and climate within species. Also known as the population average curve. Dashed lines represent a 95% confidence interval for $f_1(\text{dbh}) + \beta_0$.

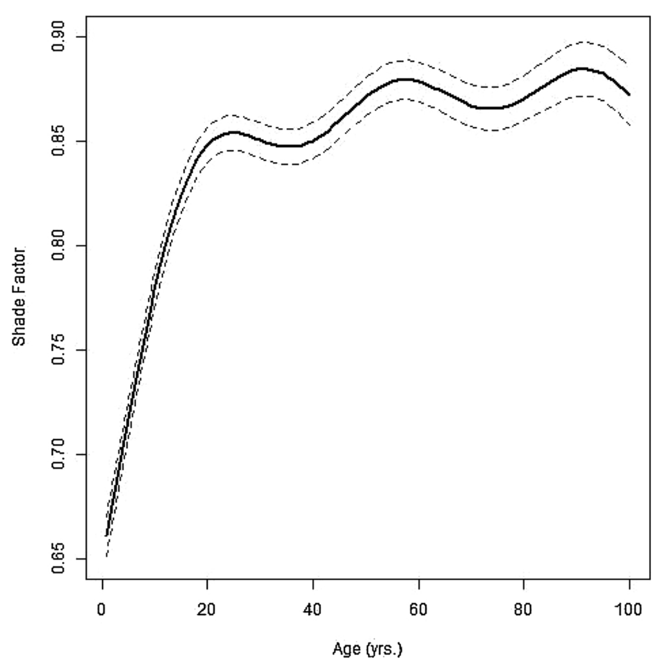

Fig. 6. Solid line is the low-rank thin-plate spline estimate of $f_2(\text{age}) + \beta_0$ from the shade factor model with age, species, and climate within species. Also known as the population average curve. Dashed lines represent a 95% confidence interval for $f_2(\text{age}) + \beta_0$.

One might assume that shade factor is related to a tree's evapotranspirational cooling effect as well as its shading effect, but this has not been tested. If a higher shade factor is due to greater leaf area density, increased evapotranspiration is likely. However, shade factors express the combined effects of foliar and non-foliar crown elements. This is not a limitation if shade factors are applied for modeling effects of tree shade on building energy use, but it is a limitation if effects on air temperatures are modeled.

Combining foliar and non-foliar elements allows for accurate parameterization of gap fraction for interception modeling, as both can impede throughfall. However, given that rain falls from above it is more desirable to obtain gap fractions from vertical images than from horizontal ones. Drone technology now makes it feasible to acquire downward-looking images for interception modeling. Differences between gap fractions from horizontal and vertical images for the same tree have not be compared, so our data for rainfall interception applications should be used with caution.

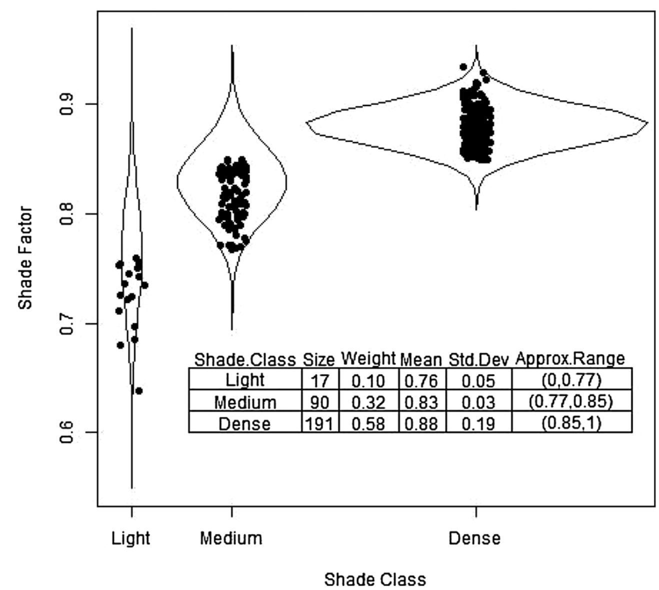

Fig. 7. Violin plots of the weighted normal mixture components (light, medium, dense) of the finite mixture model for shade class with the associated species-climate shade factors overlaid as black dots (position of dots was jittered to prevent overplotting). Also, this figure contains a table of the mean, standard deviation, and mixture weight of the normal distribution associated with each shade class, as well as the number of members (size) and the approximate shade factor range of each class.

Because non-foliar elements are included in our calculation of shade factors, their use in i-Tree regression calculations may result in overestimates of actual leaf area. As air pollutant deposition modeling relies on estimates of leaf area, use of these shade factors could result in overestimates of pollutant uptake by trees.

Our methods have a number of other limitations. Because the resolution of digital cameras increased over the 14 years data were collected, the accuracy of area calculated (i.e., pixel count) as "shaded" and "unshaded" increased as well. It is possible that this resulted in underestimates of shade factors calculated early in the study, but this cannot be tested because cameras used earlier in the study are no longer available.

Our methods do not provide good predictions of shade factor for trees older than 100 years or with dbh greater than 150 cm. This is due to limited data collected outside these values. While our method can make predictions about species/climate combinations, it is not capable of making predictions about species/climate combinations that have not been observed.

Some trees we observed were in poor health, which could influence their shade factors. We did not account for this in the model, thereby increasing variability. There were some observations that could have been outliers but were not removed because there was no justification for their removal.

Improved shade factors can increase the accuracy of modeling effects of tree shade on energy use and gap fraction on rainfall interception, but research is needed in other areas. There is a paucity of information on the duration of leaf-on and leaf-off periods for deciduous trees. Foliation period can vary substantially among species and directly influences attenuation of sunlight and interception of rainfall. Another critical variable needing further research is stem surface area, which especially influences interception and shading by deciduous trees during the leaf-off period.

4. Conclusions

For the past 30 years our estimates of tree effects on environmental services such as air pollutant uptake, building energy use, and rainfall interception have relied on a database containing a single shade factor for each of 47 species across 16 U.S. climate zones. In most cases, shade factors were obtained from measurements on a single tree in one location. The research reported here has mined a database containing 11,024 shade factors for 149 urban tree species and found that shade factors tended to increase until trees reached about 20 years or 30 cm DBH. Hence, applying a shade factor from a mature tree to a young tree of the same species is apt to overestimate actual crown density.

Our data indicate that it is not advisable to give a single shade factor for a species because shade factors are likely to change as trees age and they may change among climate zones. We provide a set of tables that contain the necessary values to compute shade factors from DBH or age with species and climate effects accounted for. This new information expands the scope of urban species with measured shade factors and allows researchers and urban foresters to more accurately predict their values across time and space.

Appendix A. Supplementary data

Supplementary data associated with this article can be found, in the online version, at https://doi.org/10.1016/j.ufug.2018.03.001.

References

ASHRAE, 1989. ASHRAE Handbook, 1989 Fundamentals. American Society of Heating, Refrigeration and Air Conditioning Engineers (ASHRAE), Atlanta, GA.
Akaike, H., 1974. A new look at the statistical model identification. IEEE Trans. Autom. Control 19 (6), 716–723.
Benaglia, T., Chauveau, D., Hunter, D.R., Young, D.S., 2009. Mixtools: an R package for analyzing mixture models. J. Stat. Softw. 32 (6), 1–29.
Berland, A., Hopton, M.E., 2014. Comparing street tree assemblages and associated stormwater benefits among commuities in metropolitan Cincinnati, Ohio USA. Urban For. Urban Green. 13, 734–741.
Burnham, K.P., Anderson, D.R., 2002. Model Selection and Multimodel Inference: A Practical Information-Theoretic Approach, 2nd edition. Springer-Verlag, New York.
Canton, M.A., Cortegoso, J.L., De Rosa, C., 1993. Solar permeability of urban trees in cities of western Argentina. Energy Build. 20, 219–230.
Dahlhausen, J., Biber, P., Rotzer, T., Uhl, E., Pretzsch, H., 2016. Three species and their space requirements in six urban environments worldwide. Forests 7 (111), 1–19. http://dx.doi.org/10.3390/f7060111.
Erley, D., Jaffe, M., 1979. Site Planning for Solar Access. (HUD-PDR-481). U.S. Superintendent of Documents, Washington, D.C.
Heisler, G.M., 1982. Reductions of solar radiation by tree crowns. Paper Presented at the American Section of the International Solar Energy Society Conference, Progress in Solar Energy.
Heisler, G.M., 1986a. Effects of individual trees on the solar radiation climate of small buildings. Urban Ecol. 9, 337–359.
Heisler, G.M., 1986b. Energy savings with trees. J. Arboric. 12 (5), 113–125.
Hwang, W.H., Wiseman, P.E., Thomas, V.A., 2015. Tree planting configuration influences shade on residential structures in four U.S. cities. Arboric. Urban For. 41 (4), 208–222.
Hwang, W.H., Wiseman, P.E., Thomas, V.A., 2016. Simulation of shade tree effects on residential energy consumption in four U.S. cities. Cities Environ. (CATE) 9 (1), 23.
Kong, F., Yin, H., James, P., Hutyra, L.R., He, H.S., 2014. Effects of spatial pattern of greenspace on urban cooling in a large metropolitan area of eastern China. Landsc. Urban Plann. 128, 35–47. http://dx.doi.org/10.1016/j.landurbplan.2014.04.018.
Kong, F., Yan, W., Zheng, G., Yin, H., Cavan, G., Zhan, W., Zhang, N., Cheng, L., 2016. Retrieval of three-dimensional tree canopy and shade using terrestrial laser scanning (TLS) data to analyze the cooling effect of vegetation. Agric. For. Meteorol. 217, 22–34.
Livesley, S.J., Baudinette, B., Glover, D., 2014. Rainfall interception and stem flow by eucalypt street trees – the impacts of canopy density and bark type. Urban For. Urban Green. 13, 192–197.
Livesley, S.J., McPherson, E.G., Calfapietra, C., 2016. The urban forest and ecosystem services: impacts on urban water, heat, and pollution cycles at the tree, street, and city scale. J. Environ. Qual. 45, 119–124.
Maco, S.E., McPherson, E.G., 2003. A practical approach to assessing structure, function, and value of street tree populations in small communities. J. Aboric. 29 (2), 84–97.
McLachlan, G.J., Peel, D., 2000. Finite Mixture Models. John Wiley & Sons, Inc, New York.
McPherson, E.G., Dougherty, E., 1989. Selecting trees for shade in the southwest. J. Arboric. 15 (2), 35–43.
McPherson, E.G., Peper, P.J., 2012. Urban tree growth modeling. Arboric. Urban For. 38, 172–180.
McPherson, E.G., van Doorn, N., Peper, P.J., 2016. Urban Tree Database and Allometric Equations. (Gen. Tech. Rpt. PSW-253). U.S. Department of Agriculture, Forest Service, Pacific Southwest Research Station, Albany, CA.
McPherson, E.G., 1984. Solar control planting design. In: McPherson, E.G. (Ed.), Energy-Conserving Site Design. American Society of Landscape Architects, Washington, D.C, pp. 141–164.
McPherson, E.G., 2010. Selecting reference cities for i-Tree Streets. Arboric. Urban For. 36 (5), 230–240.
Meng, X.L., Rubin, D.B., 1993. Maximum likelihood estimation via the ECM algorithm: a general framework. Biometrika 80 (2), 267–278.
Nowak, D.J., Crane, D., Stevens, J., Hoehn, R., Walton, J., Bond, J., 2008. A ground-based method of assessing urban forest structure and ecosystem services. Arboric. Urban For. 34 (6), 347–358.
Nowak, D.J., 1996. Estimating leaf area and leaf biomass of open-grown deciduous urban trees. For. Sci. 42 (4), 504–507.
Patterson, M.F., Wiseman, P.E., Winn, M.F., Lee, S., Araman, P.A., 2011. Effects of photographic distance on tree crown attributes calculated using UrbanCrowns image analysis software. Arboric. Urban For. 37 (4), 173–179.
Peper, P.J., McPherson, E.G., 1998. Comparison of five methods for estimating leaf area index of open-grown deciduous trees. J. Arboric. 24 (2), 98–111.
Peper, P.J., McPherson, E.G., 2003. Evaluation of four methods for estimating leaf area of isolated trees. Urban For. Urban Green. 2, 19–29.
Peper, P.J., McPherson, E.G., Mori, S.M., 2001. Equations for predicting diameter, height, crown width and leaf area of San Joaquin Valley street trees. J. Arboric. 27 (6), 306–317.
R Core Team, 2017. R: A Language and Environment for Statistical Computing. R Foundation for Statistical Computing. R Foundation, Vienna, Austria.
Rahman, M.A., Armson, D., Ennos, A.R., 2015. A comparison of the growth and cooling effectiveness of five commonly planted urban tree species. Urban Ecosyst. 18 (2), 371–389. http://dx.doi.org/10.1007/s11252-014-0407-7.
Rahman, M.A., Moser, A., Rötzer, T., Pauleit, S., 2017. Within canopy temperature differences and cooling ability of Tilia cordata trees grown in urban conditions. Build. Environ. 114, 118–128. http://dx.doi.org/10.1016/j.buildenv.2016.12.013.
Reifsnyder, W.E., Lull, H.W., 1965. Radiant Energy in Relation to Forests. (Tech. Bull. 1344). U.S. Department of Agriculture, Forest Service, Washington, D.C.
Semenzato, P., Cattaneo, D., Dainese, M., 2011. Growth prediction for five tree species in an Italian urban forest. Urban For. Urban Green. 10 (3), 169–176.
Simpson, J.R., McPherson, E.G., 1998. Simulation of tree shade impacts on residential energy use for space conditioning in Sacramento. Atmos. Environ.: Urban Atmos. 32 (1), 69–74.
Thayer, R.L., Maeda, B.T., 1985. Measuring street tree impact on solar performance: a five climate computer modeling study. J. Arboric. 11, 1–12.
Thom, J.K., Coutts, A.M., Broadbent, A.M., Tapper, N.J., 2016. The influence of increasing tree cover on mean radiant temperature across a mixed development suburb in Adelaide, Australia. Urban For. Urban Green. 20, 233–242. http://dx.doi.org/10.1016/j.ufug.2016.08.016.
Wagar, J.A., Heisler, G.M., 1986. Rating winter crown density of deciduous trees: a photographic procedure. Landsc. J. 5 (1), 9–18.
Wilkinson, D.M., Yates, D., McKennan, G.T., 1991. Light attenuation characteristics of seven common British trees. Arboric. J.: Int. J. Urban For. 15, 37–44.
Wilkinson, D.M., 1991. Can photographic methods be used for measuring the light attenuation characteristics of trees in leaf? Landsc. Urban Plann. 20, 347–349.
Wood, S.N., 2003. Thin-plate regression splines. J. R. Stat. Soc. B 65 (1), 95–114.
Wood, S.N., 2004. Stable and efficient multiple smoothing parameter estimation for generalized additive models. J. Am. Stat. Assoc. 99, 673–686.
Wood, S.N., 2006. Generalized Additive Models: An Introduction with R. Chapman and Hall/CRC, Boca Raton, Florida.
Wood, S.N., 2011. Fast stable restricted maximum likelihood and marginal likelihood estimation of semiparametric generalized linear models. J. R. Stat. Soc. 73 (1), 3–36.
Wood, S.N., 2016. Just another gibbs additive modeler: interfacing JAGS and mgcv. J. Stat. Softw. 75 (7), 1–15. http://dx.doi.org/10.18637/jss.v075.i07.
Xiao, Q., McPherson, E.G., Simpson, J.R., Ustin, S.L., 1998. Rainfall interception by Sacramento's urban forest. J. Arboric. 24 (4), 235–244.
Xiao, Q., McPherson, E.G., Ustin, S.L., Grismer, M.E., 2000. A new approach to modeling tree rainfall interception. J. Geogr. Res. Atmos. 105, 29173–29188.
Yoon, T.K., Park, C.-W., Lee, S.J., Ko, S., Kim, K.N., Son, Y., Lee, K.H., Oh, S., Lee, W.-K., Son, Y., 2013. Allometric equations for estimating the aboveground volume of five common urban street tree species in Daegu, Korea. Urban For. Urban Green. 12 (3), 344–349.
Zölch, T., Henze, P., Keilholz, P., Pauleit, S., 2017. Regulating urban surface runoff through nature-based solutions – an assesment at the micro-scale. Environ. Res. 157, 135–144.